Proceedings of the Online Conference "Applications of Physics in Mechanical and Material Engineering"

Numerical Modeling of Shrinkage Cavity Formation Process in Cast Steel Support

T. Skrzypczak*, E. Węgrzyn-Skrzypczak and L. Sowa

Częstochowa University of Technology, 42-201 Częstochowa, Poland

Doi: 10.12693/APhysPolA.139.487
*e-mail: tomasz.skrzypczak@pcz.pl

The presented work is focused on the numerical modeling of a solidification process of a support made of cast steel in a permanent mould. The shrinkage cavity formation phenomenon is taken into account due to its importance in the casting process. The formation process of the internal macroscopic voids due to the volumetric shrinkage of the solidifying material is a common and serious concern of the casting process. Governing equations of the mathematical and numerical models are presented. The numerical approach of the considered problem is based on the finite element method (FEM). The algorithm of the shrinkage cavity creation process is described. The numerical procedure of the macroscopic defect formation is based on the recognition of the isolated liquid volumes where the amount of shrinkage is computed in each time step. The recognition is performed by the selection of the interconnected nodes filled with liquid in the finite element mesh. On the basis of the numerical model, an original computer program was made. The numerically obtained location and shape of the macroscopic defects were compared to the shrinkage cavity in the real casting.

topics: solidification, shrinkage cavity, numerical modeling, finite element method

1. Introduction

Technological processes such as casting take into account various thermal phenomena. Casting is a technological process in which a liquid metal solidifies in a mould made of sand or cast iron. Between the casting and the mould, heat is transported through the gap filled with gas. The presented work considers a gap of the constant width. The formation of the casting is accompanied by the contraction of the liquid and solid phases due to a cooling process. Shrinking is also observed during the liquid-solid phase transformation between liquidus and solidus temperatures. Contraction in a different part of the casting due to temperature decreasing is the reason of the micro- and macroscopic defects formation. The most common macroscopic defects are conical pipe shrinkages located in the top of the riser and also closed voids observed deeper in the casting [1, 2]. Such defects are called "shrinkage cavities."

The presented paper focuses on the formation process of macroscopic defects and neglects micropores. Macropores can be scattered in the casting depending on its geometry, the shape and size of the riser and the cooling conditions. The shrinkage cavity formation and numerical modeling of this phenomenon is widely investigated [1–8].

Casting formation can be divided into three stages. The first stage starts at pouring the molten metal into the mould and ends at the moment of appearing of the first grain of the solid phase. This stage affects the formation of pipe shrinkages due to the contraction of the liquid phase. The next stage is the solidification process occurring between the liquidus and solidus temperatures. The contraction of the material is caused by the liquid–solid phase change and is taken into account in the numerical model in the procedure of shrinkage cavities formation. The amount of volume loss depends on the difference between the densities of the liquid and solid phases. Depending on the geometry of the casting and the riser, the macropores filled with gas can be located only in the riser or in the riser and the casting.

The third stage starts at the end of solidification. The contraction of the material is caused by the cooling process of the solid material. It lasts till the shakeout operation and is neglected in the model.

2. Mathematical and numerical descriptions

Figure 1 shows the casting-mould system divided into two parts Ω_1 and Ω_2. There, Ω_1 is the casting with the riser initially filled with the liquid steel while Ω_2 is the mould made of cast iron.

The external surfaces of the casting and the mould are denoted as Γ_1 and Γ_2, respectively. Between the casting and the mould, the gap of constant width d filled with gas is observed.

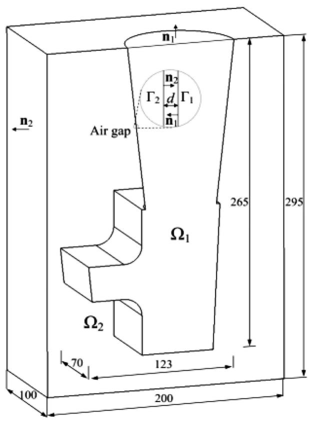

Fig. 1. Scheme of the casting-mould system (dimensions in mm).

A mathematical model for the considered process relies on the description of transient heat transport in the casting-mould system. Namely,

$$\frac{\partial}{\partial x}\left(\lambda_1\frac{\partial T^{(1)}}{\partial x}\right)+\frac{\partial}{\partial y}\left(\lambda_1\frac{\partial T^{(1)}}{\partial y}\right) +\frac{\partial}{\partial z}\left(\lambda_1\frac{\partial T^{(1)}}{\partial z}\right)=c^*\rho_1\frac{\partial T^{(1)}}{\partial t} \quad (1)$$

$$\frac{\partial}{\partial x}\left(\lambda_2\frac{\partial T^{(2)}}{\partial x}\right)+\frac{\partial}{\partial y}\left(\lambda_2\frac{\partial T^{(2)}}{\partial y}\right) +\frac{\partial}{\partial z}\left(\lambda_2\frac{\partial T^{(2)}}{\partial z}\right)=c_2\rho_2\frac{\partial T^{(2)}}{\partial t}, \quad (2)$$

where T is the temperature [K], λ represents the coefficient of heat conduction [J/(s m K)], c represents the specific heat [J/(kg K)], c^* is the specific heat modified by the heat [J/(kg K)] released during solidification, ρ is the density [kg/m^3], (x, y, z) are the spatial coordinates [m], t represents time [s], while the respective superscripts '1' and '2' indicate the casting and the mould.

Effective specific heat c^* is defined as [9]:

$$c^*=\begin{cases} c_s, & T<T_S\\ \frac{1}{2}(c_s+c_l)+\frac{L}{T_L-T_S}, & T_S\le T\le T_L,\\ c_l, & T>T_L\end{cases} \quad (3)$$

where T_S, T_L are the solidus and liquidus temperatures [K], c_s and c_l are the specific heat of the solid and liquid phase [J/(kg K)] and L denotes the latent heat of solidification [J/kg].

The additional conditions are needed to fully describe the mathematical model. Let us assume the following:

$$-\lambda_1\frac{\partial T^{(1)}}{\partial n_1}=\alpha_1\left(T^{(1)}-T^{(1)}_\infty\right),$$

$$-\lambda_2\frac{\partial T^{(2)}}{\partial n_2}=\alpha_2\left(T^{(2)}-T^{(2)}_\infty\right) \quad (4)$$

$$-\lambda_2\frac{\partial T^{(2)}}{\partial n_2}=\frac{\lambda_{\mathrm{g}}}{d}\left(T^{(2)}-T^{(1)}\right)=\lambda_1\frac{\partial T^{(1)}}{\partial n_1} \quad (5)$$

and

$$T^{(1)}(t=0)=T^{(1)}_0,\quad T^{(2)}(t=0)=T^{(2)}_0, \quad (6)$$

where α is the heat transfer coefficient [J/(sm^{2}K)], T_∞ represents the ambient temperature [K], n describes the direction of the vector in the direction normal to the external surface. Next, λ_{g} is the coefficient of heat conduction in the gap [J/(s m K)], d is the width of the gap [m], and T_0 represents the initial temperature distribution [K].

The standard Galerkin formulation with the Euler backward time integration scheme are used to derive a global set of equations:

$$\left(K_1+\frac{1}{\Delta t}M_1\right)\boldsymbol{T}_1^{f+1}=\boldsymbol{B}_1+\frac{1}{\Delta t}M_1\boldsymbol{T}_1^{f}, \quad (7)$$

$$\left(K_2+\frac{1}{\Delta t}M_2\right)\boldsymbol{T}_2^{f+1}=\boldsymbol{B}_2+\frac{1}{\Delta t}M_2\boldsymbol{T}_2^{f}, \quad (8)$$

where K_1, K_2 represents the matrices of heat conductivity, M_1, M_2 are the matrices of heat capacity, $\boldsymbol{B}_1$, $\boldsymbol{B}_2$ are the vectors containing boundary conditions, f is the number of the current time step and Δt is the time step [s].

The numerical calculations were based on solving (7) and (8) independently to fulfill condition (5) (heat fluxes on both sides of the gap must be the same) with the use of the iterative procedure for each time step. The separated finite element meshes were involved in this operation. The procedure of the shrinkage cavities formation was the next important step in the calculations. Figure 2 shows the algorithm of the solidification process containing shrinkage cavities development.

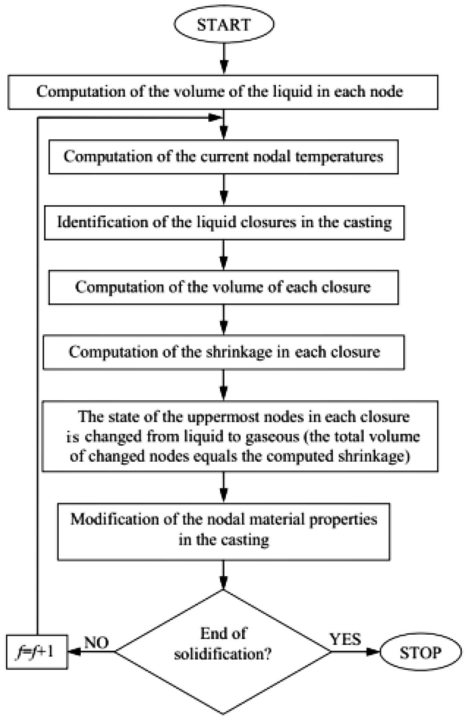

Fig. 2. Algorithm of the solidification process with shrinkage cavities formation.

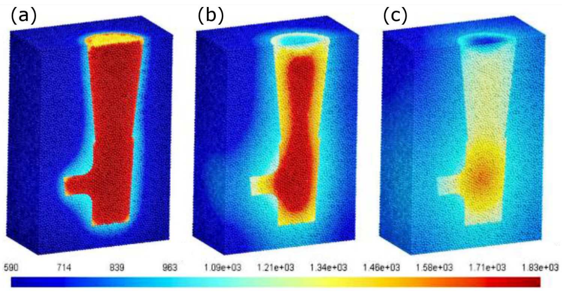

Fig. 3. Temperature distribution in the casting and the mould at 25 s (a), 100 s (b), 200 s (c).

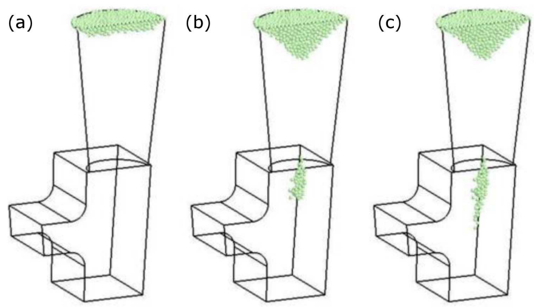

Fig. 4. Localization of the shrinkage cavities in the casting at 25 s (a), 100 s (b), 200 s (c).

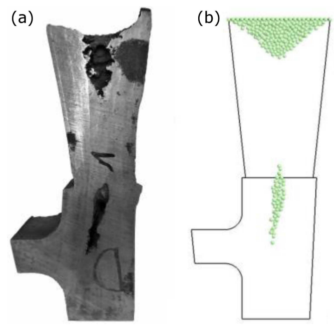

Fig. 5. Localization of the shrinkage cavities in the real casting (a) and the results of numerical computations (b).

Each node initially contains a certain amount of liquid material. During solidification, a solid phase appears, thus the number of nodes containing pure liquid decreases. One or more liquid closures can be observed as the solidification evolves. Shrinkage of the solidifying material in each closure leads to the formation of internal voids filled with a gaseous medium. In each time step, the current shape and position of each closure must be actualized and the state of a certain number of nodes must be changed from liquid to gaseous. The contraction of the material during liquid–solid phase transformation depends on the shrinkage coefficient S_h. Starting from the highest node (nodes are sorted according to their vertical coordinate), in each liquid closure the liquid phase is replaced by the air. The calculation process is stopped when the entire material turns into the solid. More details of the procedure of shrinkage cavities formations are described in [10].

3. Example of calculation

The original computer program was developed to model the described process. Material properties of the casting are taken from [10] while the properties of the mould and gas in the gap and shrinkage cavities are taken from [11].

The molten steel of initial temperature of 1833 K is poured into the mould of initial of temperature 600 K. The pouring stage and motion of the liquid metal are neglected. Due to the symmetry, only one half of the casting-mould system is considered with thermal insulation condition assumed on the plane of symmetry. The convective heat transfer is defined on the external boundaries of the mould and on the top of the casting with the heat transfer coefficient $\alpha = 20$ J/(s m^{2}K) and the ambient temperature $T_\infty = 300$ K. The time step is constant $\Delta t = 0.25$ s. Between the casting and the mould, the gas gap of the constant width $d = 0.001$ m and heat conductivity $\lambda_g = 1$ J/(s m K) are assumed. The geometries and the meshes are prepared with the use of a GMSH preprocessor [12]. The meshes for the casting and the mould are built of tetrahedrons and contain 15212 and 65539 nodes, respectively.

The solidification process lasted about 180 s. Figure 3 shows the temperature distribution in the early stage of solidification (Fig. 3a), in the middle of the process (Fig. 3b) and at its end (Fig. 3c).

Figure 4 shows three stages of the formation process of macroscopic defects in the casting. A conical pipe shrinkage is visible in the upper part of the riser but more undesirable defect is located deeper below the riser (Fig. 4b and c). The comparison of real defects in the support with the results of numerical modeling is presented in Fig. 5. The calculated localizations of the shrinkage cavities are comparable to the positions of the real defects in the casting.

4. Conclusions

The presented results of numerical modeling of the solidification process of the steel support in the permanent mould show acceptable agreement with the technological practice. the described approach is useful for predicting multiple macroscopic cavities. The original computer program created with the use of FEM is effective and robust for complex three-dimensional geometries. The developed solver is also free and easier to modify than expensive commercial packages. It can be useful for predicting macroscopic defect formation before the start of the casting process. Future work is focused on the modeling of micropores formation to improve the model in prediction of defects formation.

References

[1] Ch. Pequet, M. Rappaz, M. Gremaud, *Metall. Mater. Trans. A* **33**, 2095 (2002).

[2] J. Hajkowski, P. Roquet, M. Khamashta, E. Codina, Z. Ignaszak, *Arch. Foundry Eng.* **17**, 57 (2017).

[3] M.C. Flemings, *The solidification processing*, McGraw-Hill, New York 1974.

[4] C.J. Kim, S.T. Ro, *J. Heat. Trans.* **115**, 1078 (1993).

[5] J. Campbell, *Castings* (2nd ed.), Butterworth-Heinemann, Oxford 2003.

[6] C. Zhang, Y. Bao, M. Wang, L. Zhang, *Arch. Foundry Eng.* **16**, 27 (2016).

[7] A.S. Jabur, F.M. Kushnaw, *J. Appl. Computat. Math.* **6**, 7 (2017).

[8] M. Wu, A. Ludwig, A. Kharicha, *Appl. Math. Model.* **41**, 102 (2017).

[9] B. Mochnacki, J.S. Suchy, *Numerical Methods in Computations of Foundry Processes*, Kraków: Polish Foundrymen's Technical Association, Kraków 1993.

[10] T. Skrzypczak, L. Sowa, E. Węgrzyn-Skrzypczak, *Arch. Foundry Eng.* **20**, 37 (2020).

[11] T. Skrzypczak, E. Węgrzyn-Skrzypczak, L. Sowa, *Arch. Foundry Eng.* **17**, 147 (2017).

[12] C. Geuzaine, J.F. Remacle, *Int. J. Numer. Meth. Eng.* **79**, 13091 (2009).